

Logarithmic corrections and soft photon phenomenology in the multipole model of the nucleon form factors

G. Vereshkov and O.Lalakulich^a

Research Institute of Physics, Southern Federal University, 344090 Rostov-on-Don, Russia

Abstract. We analyzed the presently available experimental data on nucleon electromagnetic form factors within a multipole model based on dispersion relations. A good fit of the data is achieved by considering the coefficients of the multipole expansions as logarithmic functions of the momentum transfer squared. The superconvergence relations, applied to this coefficients, makes the model agree with unitary constraints and pQCD asymptotics for the Dirac and Pauli form factors. The soft photon emission is proposed as a mechanism responsible for the difference between the Rosenbluth, polarization and beam-target-asymmetry data. It is shown, that the experimentally measured cross sections depend not only on the Dirac and Pauli form factors, but also on the average number of the photons emitted. For proton this number is shown to be different for different types of experimental measurements and then estimated phenomenologically. For neutron the same mechanism predicts, that the data from different types of experiments must coincide with high accuracy. A joint fit of all the experimental data reproduce the Q^2 -dependence with the accuracy $\chi^2/dof = 0.86$. Predictions of the model, that 1) the ratios of the proton form factors G_E/G_M are different for Rosenbluth, polarization and beam-target-asymmetry experiments and 2) similar ratios are nearly the same for neutron, can be used for experimental verification of the model.

PACS. 25.30.Bf Elastic electron scattering – 13.40.Gp Electromagnetic form factors

1 Introduction

The nucleon elastic form factors are of fundamental importance for understanding the electromagnetic structure of the nucleon. Until recently they only have been measured through Rosenbluth technique in experiments on non-polarized elastic electron-nucleon scattering. This method gives non-interfering electric G_{Ep} , G_{En} and magnetic G_{Mp} , G_{Mn} form factors for proton and neutron, respectively.

Recent progress in experimental technique made it possible to use polarized beams and/or polarized targets, which brings two new methods [1], polarization transfer and beam-target asymmetry, to determine the ratio of the electric to magnetic form factors.

New experimental data, recently obtained by these methods, show an excellent agreement with the old Rosenbluth data at low momentum transfer, $Q^2 \lesssim 1 \text{ GeV}^2$, and posed intriguing questions at higher Q^2 .

Proton electric and magnetic form factors, normalized on the dipole function $G_D = (1 - t/0.71)^{-2}$, as they are determined with the Rosenbluth technique are shown in Fig. 1. The ratios of proton form factors, as they are determined from different experimental techniques are shown in Fig. 2. Neutron electric and magnetic form factors, also normalized on the dipole function $G_D = (1 - t/0.71)^{-2}$,

come from the Rosenbluth and polarization transfer techniques and are shown in Fig. 3. The ratio of the neutron form factors, as it is determined from polarization data is shown in Fig. 4. Fit of these data within the framework of the model, proposed in this paper, is shown by solid lines. The references on the original experiments are summarized in Tables 1,2 (see page 11, also [2,3] for earlier compilations).

In Figs. 1, 2, 3 we use logarithmic scale for Q^2 . This way one could easily notice, that

(i) in the whole experimentally investigated Q^2 region the global Q^2 -evolution of the form factors $G_E^{(Ros)}$, $G_{Mp}^{(Ros)}$, $G_{Mn}^{(Ros)}$, obtained via the Rosenbluth extraction is described by the dipole model with an accuracy of about 10 – 20 %;

(ii) deviations from the dipole model are of logarithmic form;

(iii) The ratio of the proton form factors $R_p^{(pol)} = \mu_p G_{Ep}^{(pol)} / G_{Mp}^{(pol)}$, measured in the polarization transfer experiments, steeply falls down as Q^2 increases up to 5.55 GeV^2 . The ratio $R_p^{(Ros)} = \mu_p G_{Ep}^{(Ros)} / G_{Mp}^{(Ros)}$, calculated from Rosenbluth data is approximately constant. This is illustrated in Fig.2, which also includes data from beam-target asymmetry experiments. Thus, recoil polarization measurements contradict the Rosenbluth measurements and there is a

^a *Present address:* Department of Subatomic and Radiation Physics, Ghent University, Ghent

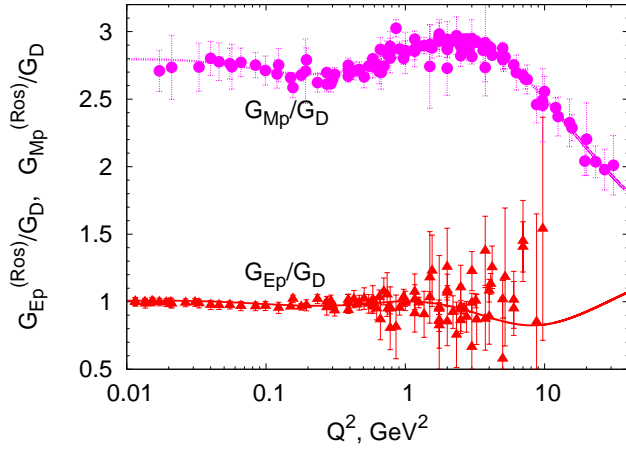


Fig. 1. Proton form factors, obtained by Rosenbluth separation technique, normalized on the dipole function $G_D = (1 + Q^2/0.71)^{-2}$

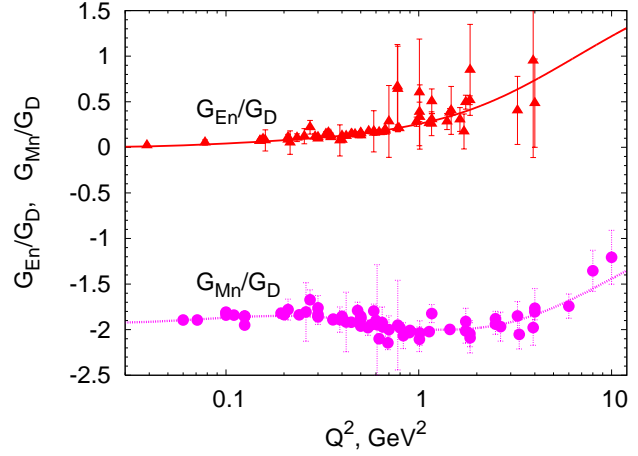


Fig. 3. Neutron form factors, normalized on the dipole function $G_D = (1 + Q^2/0.71)^{-2}$

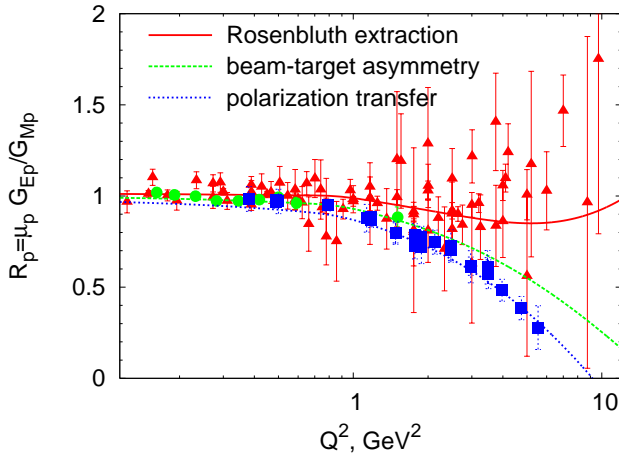


Fig. 2. Ratio of the proton form factors, obtained with different experimental techniques

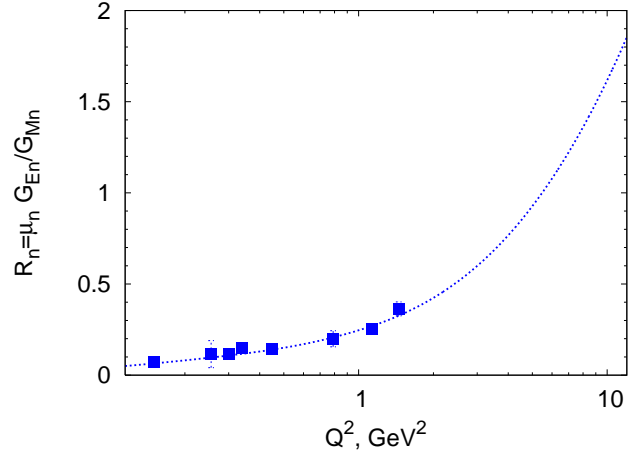


Fig. 4. Ratio of the neutron form factors

dramatic problem to make them agree with each other [4].

Phenomenological fit of the form factors without discussing their physical nature is available in Refs. [5,6,7]. Theoretically the form factors are investigated within different models (their classification, short review and references see in [8][Section V]).

1. In low Q^2 region a good description of the data is provided in the constituent quark models, including cloudy bag and diquark models. These models rely on the spectroscopic data to fix their free parameters and then provide predictions for the nucleon form factors (see [8] for a short review).

2. In high Q^2 region ($Q^2 > 20-30 \text{ GeV}^2$ for form factor problem) perturbative QCD gains its power, which makes it possible to calculate the pQCD asymptotics for $F_{1n,p}$ [9, 10] and $F_{2p,n}$ [11,12] from pure theoretical considerations.

3. An attempt to extend these calculations to a lower- Q^2 region was recently made by Guidal *et. al* [13] in a model, based on nonperturbative generalised parton dis-

tributions. This model contains free parameters, which are adjusted to fit the data on the form factors.

4. The models at the nucleon-meson level by construction intend to describe the data in both low- and high- Q^2 regions. Complying with the low- Q^2 and pQCD asymptotics of the form factors must be inevitable feature of such models. In vector meson dominance models [14,15, 16,17,18] the photon couples to the nucleon via vector mesons; to date four different vector mesons are used in such models;

5. In a model of Mainz-Bonn-Jülich group [19,20,21], based on the dispersion-theoretical analysis, some poles of the multipole expansions are also related to the vector meson masses. In addition the effect of many-meson exchange is taken into account. In this approach at least three isovector and three isoscalar mesons must be considered in order to fit all the data.

Different approaches to the physical nature of the form factors are complementary, supporting the idea of quark-hadron duality. It is known nowadays, that the effective theory of hadronic fields can be derived from QCD. This advances the idea of a univocal correspondence between

the quark and nucleon–meson models of the form factors. At present, however, such correspondence can hardly be traced, because the calculations in nonperturbative QCD are too complicated as well as the final form of the nucleon–meson phenomenology is not yet established.

In this situation we base our model on two the most reliable general consequences of the field theory. They are: (i) the multipole structure of the form factors, which is predicted by the dispersion relations [22,23]; (ii) the asymptotical behavior of the Dirac and Pauli form factors, calculated in perturbative QCD [9,10,11,12].

In Section 2 we introduce our formalism and establish the full set of superconvergence relations imposed on the coefficients of the multipole expansions in order to adjust the multipole form factors with the QCD asymptotics and unitarity constraints. As we have already mentioned, a similar approach was first used in the dispersion–theoretical analysis of the nucleon form factors developed by Mainz–Bonn–Jülich group [19,20,21] since 1996. We keep the same lines, but use improved logarithmic dependences of the multipole coefficients. Instead of one universal logarithmic function for the pole contributions and two more for the two-pion continuum in the Mainz–Bonn–Jülich model, we introduce four functions with leading and subleading logarithms, which are motivated by the modern pQCD asymptotics. This approach allows us to make all the poles correspond to the masses of the physical mesons in the PDG tables, as well as to achieve a better fit of the data.

Another purpose of the paper is to resolve the above described discrepancy in the proton form factors and propose a way to reconcile the three sets of data. Up to now this question remained open in all the above cited models, where fits have to be based on the recoil polarization data, practically ignoring the high- Q^2 Rosenbluth data. Much attention in this respect was devoted to the radiative corrections [24] and in particular to the two-photon exchange [25,26,27] mechanisms. An approach taking into account the hadronic contribution to the electron structure functions is presented in [28]. A global analysis of the Rosenbluth data [29] found, however, hardly ever evidence for the two-photon exchange effects. We propose, that the physical phenomena responsible for the discrepancy is the soft photon emission, which proceeds differently in different types of experiments.

In Section 3 we argue, that in electron–nucleon scattering, the soft photons that are not detected experimentally can be emitted, and this effect influence the values of the experimentally measured electric and magnetic form factors and their ratios. It is shown that the observables, extracted from the cross sections, depend not only on the Dirac and Pauli form factors, but also on the average number of the photons emitted. This dependence results from the fact [30], that the Dirac and Pauli form factors contribute to the emission of photons differently. In the polarization transfer experiments only events without photon emission are experimentally possible, because otherwise the photon would carry away the angular momentum and thus prevent the transfer of polarization. Non-polarized

electrons in the final states, on the other hand, are inevitably accompanied by soft photon emission. We provide formulas for the observable values in all the three types of experiments.

Section 4 is devoted to the numerical analysis. The joint fits of all experimental data available is performed according to the formulas presented in the previous sections. The agreement between the theory and the experimental data is achieved at the level $\chi^2/dof = 0.86$. In Section 5 we give our predictions, which can be used for the experimental verification of the model and in Section 6 we summarize our findings.

2 Multipole model for Dirac and Pauli form factors.

2.1 Formulation of the model

The main contribution to the dispersion–relation form factors is given by multipole expansion, which accounts for one–meson exchange in the approximation of the narrow meson width. Retaining the isotopic symmetry, the most general structure for the form factors at $t = -Q^2 < 0$ is:

$$\begin{aligned} F_{1p,n}(t) &= Q_{p,n}(t) - \frac{1}{2} \left[\sum_{k=1}^{N_s} a_{s(k)}(t) \pm \sum_{k=1}^{N_v} a_{v(k)}(t) \right] + \\ &+ \frac{1}{2} \left[\sum_{k=1}^{N_s} \frac{a_{s(k)}(t)m_{s(k)}^2}{m_{s(k)}^2 - t} \pm \sum_{k=1}^{N_v} \frac{a_{v(k)}(t)m_{v(k)}^2}{m_{v(k)}^2 - t} \right], \\ F_{2p,n}(t) &= \mu_{p,n}^{(an)}(t) - \frac{1}{2} \left[\sum_{k=1}^{N_s} b_{s(k)}(t) \pm \sum_{k=1}^{N_v} b_{v(k)}(t) \right] + \\ &+ \frac{1}{2} \left[\sum_{k=1}^{N_s} \frac{b_{s(k)}(t)m_{s(k)}^2}{m_{s(k)}^2 - t} \pm \sum_{k=1}^{N_v} \frac{b_{v(k)}(t)m_{v(k)}^2}{m_{v(k)}^2 - t} \right]. \end{aligned} \quad (1)$$

Here N_v and N_s are, correspondingly, the numbers of isotriplet and isosinglet poles of the scattering amplitude. The upper and the lower signs correspond to proton and neutron, respectively.

Generally the phenomenology of the dispersion relations allows for the coefficients of the multipole expansions $Q_{p,n}(t)$, $\mu_{p,n}^{(an)}(t)$, $a_{s,v(k)}(t)$, $b_{s,v(k)}(t)$ to be slow variable (logarithmic) functions of t . At $-t \rightarrow 0$ the limiting values of functions $Q_{p,n}(t)$, $\mu_{p,n}^{(an)}(t)$ are equal to the charges and anomalous magnetic moments of nucleons:

$$\begin{aligned} Q_p(0) &= 1, & \mu_p^{(an)}(0) &\equiv \mu_p - 1 = 1.793, \\ Q_n(0) &= 0, & \mu_n^{(an)}(0) &\equiv \mu_n = -1.913. \end{aligned} \quad (2)$$

The asymptotical behavior of the Dirac and Pauli form factors at $-t \rightarrow \infty$ traces back to the results of the per-

turbative QCD:

$$\begin{aligned} F_{1p,n}(t) &\rightarrow \left(\frac{4M_N^2}{t}\right)^2 \frac{C_{1p,n}}{\ln^{p_1}|t|/\Lambda^2}, \\ F_{2p,n}(t) &\rightarrow \left(\frac{4M_N^2}{t}\right)^3 \frac{C_{2p,n}}{\ln^{p_2}|t|/\Lambda^2}, \\ p_1 &= 2 + \frac{32}{9\beta}, \quad p_2 = \frac{8}{3\beta}, \quad \beta = 11 - \frac{2}{3}n_f. \end{aligned} \quad (3)$$

where $\Lambda \simeq 300$ MeV is the QCD scale. The exponent p_1 is calculated theoretically and is known with rather good accuracy; the constants $C_{1p,n}$ are to be evaluated by comparing the experimental data with the parton model [9, 10, 12]. The asymptotic of the Pauli form factor from Eq. (3) and the constants $C_{2p,n}$ are evaluated in [11]. Another asymptotic is proposed in [12].

The power dependence of the asymptotics in Eq. (3) results from the quark counting rules [31, 9]. Those in turn follow from the analysis of the process with the quark momentum redistribution among the quark and gluon components of the nucleon. The logarithmic functions describe the renormalization of the color charge and the wave functions of the partons. Note, that in the elastic scattering theory the region of the perturbative QCD applicability is estimated differently than in the deep inelastic scattering. We discuss this question in the next paragraph before proceeding with the form factors.

In DIS the perturbative description of the inclusive processes is possible, if for the initial act of the electron-parton interaction the inequality $|t| \gg T_g^{-2}$ is satisfied, with $T_g \simeq (1.5 \text{ GeV})^{-1}$ being the correlation length (the characteristic scale) of the nonperturbative gluon fluctuations. In case of the elastic eN -scattering the momentum, transferred to one proton in the initial interaction act, is uniformly distributed among all partons; and in the region of QCD applicability all processes of momentum redistribution must be hard. The number of partons, participating in these processes, is no less than the number of the valent quarks $n_q = 3$, so the perturbative description of the elastic scattering is only justified for $|t| \gg |t_{QCD}|$, with $|t_{QCD}| \simeq n_q T_g^{-2} \simeq 7 \text{ GeV}^2$. Among the experimental data available, only the proton magnetic form factor at $|t| = 20 - 30 \text{ GeV}^2$ could probably be compared with the perturbative QCD. However, the very fact that the QCD asymptotics (3) exist is of fundamental importance at discussing the general mathematical structure of the form factors.

2.2 The Superconvergence Relations

Thus, multipole form factors (1) must satisfy the asymptotics (3), which automatically include the unitarity conditions. In this way one phenomenologically accounts for the QCD effects at the valence quark level, that is (i) the redistribution of the transferred momentum between quarks, (ii) subsiding of chromodynamical interactions as Q^2 increases, (iii) dependence of parton (valence quark) distribution functions on Q^2 .

There are two ways to satisfy pQCD asymptotics. One can nullify the non-pole terms in the expansion (nullify the so called "nucleon core") and impose the corresponding conditions to each of the coefficients $a_{s,v(k)}(t)$, $b_{s,v(k)}(t)$ by modelling them by pow-low and logarithmic functions. This way is used in Refs. [15, 16].

Another way is to satisfy the pow-low asymptotics by imposing the "superconvergence relations", as they are referred to in the papers of the Mainz-Bonn-Julich group, over the whole sets of the multipole coefficients, so that they relate parameters of the different poles to each other. The multipole coefficients in these papers are considered as logarithmic functions with the leading logarithms only.

The same approach was taken later by Bratislava group in [32], who use the term "asymptotic conditions". The logarithmic dependences of the multipole coefficients are, however, ignored in the papers of this group, which makes a good fit of the experimental data difficult.

We implement the latter way and impose the superconvergence relations (SR) on the four sets of our coefficients $a_{s,v(k)}(t)$, $b_{s,v(k)}(t)$. Let us expand Eq. (1) on powers $1/t$ and nullify the terms of the order t^0 , t^{-1} for $F_{1p,n}$ and t^0 , t^{-1} , t^{-2} for $F_{2p,n}$. Since isovector and isoscalar modes are independent, there are 10 independent SR:

$$\begin{aligned} \sum_{k=1}^{N_{s,v}} a_{s,v(k)}(t) &= q_{s,v}(t), & \sum_{k=1}^{N_{s,v}} a_{s,v(k)}(t) m_{s,v(k)}^2 &= 0, \\ \sum_{k=1}^{N_{s,v}} b_{s,v(k)}(t) &= (\mu_p \pm \mu_n - 1) \mu_{s,v}(t), \\ \sum_{k=1}^{N_{s,v}} b_{s,v(k)}(t) m_{s,v(k)}^2 &= 0, & \sum_{k=1}^{N_{s,v}} b_{s,v(k)}(t) m_{s,v(k)}^4 &= 0, \end{aligned} \quad (4)$$

where

$$q_{s,v}(t) \equiv Q_p(t) \pm Q_n(t), \quad \mu_{s,v}(t) \equiv \frac{\mu_p^{(an)}(t) \pm \mu_n^{(an)}(t)}{\mu_p \pm \mu_n - 1}. \quad (5)$$

The upper and lower signs here correspond to the isoscalar (s) and isovector (v) parts, respectively. The SR (4) and the normalization conditions (2) allow us to attribute the t dependence of the coefficients $a_{s,v(k)}(t)$, $b_{s,v(k)}(t)$ to the four phenomenological logarithmic functions $q_{s,v}(t)$, $\mu_{s,v}(t)$ (which do not depend on k) and introduce new parameters $\tilde{a}_{s,v(k)}$, $\tilde{b}_{s,v(k)}$:

$$\begin{aligned} a_{s,v(k)}(t) &= q_{s,v}(t) \tilde{a}_{s,v(k)}, \\ b_{s,v(k)}(t) &= (\mu_p \pm \mu_n - 1) \mu_{s,v}(t) \tilde{b}_{s,v(k)}. \end{aligned}$$

In terms of these parameters the SR are reduced to the following expressions:

$$\begin{aligned} \sum_{k=1}^{N_{s,v}} \tilde{a}_{s,v(k)} &= 1, & \sum_{k=1}^{N_{s,v}} \tilde{a}_{s,v(k)} m_{s,v(k)}^2 &= 0, \\ \sum_{k=1}^{N_{s,v}} \tilde{b}_{s,v(k)} &= 1, & \sum_{k=1}^{N_{s,v}} \tilde{b}_{s,v(k)} m_{s,v(k)}^2 &= 0, \\ \sum_{k=1}^{N_{s,v}} \tilde{b}_{s,v(k)} m_{s,v(k)}^4 &= 0. \end{aligned} \quad (6)$$

The form of the functions $q_{s,v}(t)$ and $\mu_{s,v}(t)$ will be discussed in the next subsection and finally given in Eq. (12).

Notice, that SR (6) are independent of the kinematic variable t , so the values $\tilde{a}_{s,v(k)}$, $\tilde{b}_{s,v(k)}$ can be considered as numbers. It is also important, that three SR for the parameters $\tilde{b}_{v(k)}$ are only compatible with three or more isovector and isoscalar mesons. Applying SR (6) to the form factors (1) makes the non-pole terms (the first and the second terms) vanish and results in:

$$\begin{aligned} F_{1p,n}(t) &= \frac{1}{2} \left[q_s(t) \sum_{k=1}^{N_s} \frac{\tilde{a}_{s(k)} m_{s(k)}^2}{m_{s(k)}^2 - t} \pm q_v(t) \sum_{k=1}^{N_v} \frac{\tilde{a}_{v(k)} m_{v(k)}^2}{m_{v(k)}^2 - t} \right], \\ F_{2p,n}(t) &= \frac{1}{2} \left[(\mu_p + \mu_n - 1) \mu_s(t) \sum_{k=1}^{N_s} \frac{\tilde{b}_{s(k)} m_{s(k)}^2}{m_{s(k)}^2 - t} \pm \right. \\ &\quad \left. \pm (\mu_p - \mu_n - 1) \mu_v(t) \sum_{k=1}^{N_v} \frac{\tilde{b}_{v(k)} m_{v(k)}^2}{m_{v(k)}^2 - t} \right]. \end{aligned} \quad (7)$$

2.3 Logarithmic corrections

For the logarithmic functions (5) their limit values at $-t \rightarrow 0$ can be derived from (2). Their pQCD asymptotics at $-t \rightarrow \infty$ follow from (3):

$$\begin{aligned} q_{s,v}(t) &\rightarrow \begin{cases} 1, & -t \rightarrow 0, \\ \frac{C_{1s,v}}{\ln^{p_1} |t|/\Lambda^2}, & -t \rightarrow \infty, \end{cases} \\ \mu_{s,v}(t) &\rightarrow \begin{cases} 1, & -t \rightarrow 0, \\ \frac{C_{2s,v}}{\ln^{p_2} |t|/\Lambda^2}, & -t \rightarrow \infty, \end{cases} \end{aligned} \quad (8)$$

where $C_{js,v}$ will be derived below and given in Eq.(11)

Making an asymptotic expansion of (7) and using (8) one gets at $-t \rightarrow \infty$ the following asymptotics of the form factors:

$$\begin{aligned} F_{1p,n}(t) &\rightarrow -\frac{1}{2t^2 \ln^{p_1} |t|/\Lambda^2} \left[C_{1s} \sum_{k=1}^{N_s} \tilde{a}_{s(k)} m_{s(k)}^4 \right. \\ &\quad \left. \pm C_{1v} \sum_{k=1}^{N_v} \tilde{a}_{v(k)} m_{v(k)}^4 \right] \end{aligned}$$

$$= -\frac{16M_N^4}{2t^2 \ln^{p_1} |t|/\Lambda^2} [C_{1s} \kappa_{1s} \pm C_{1v} \kappa_{1v}],$$

$$\begin{aligned} F_{2p,n}(t) &\rightarrow \frac{-1}{2t^3 \ln^{p_2} |t|/\Lambda^2} \left[(\mu_p + \mu_n - 1) C_{2s} \sum_{k=1}^{N_s} \tilde{b}_{s(k)} m_{s(k)}^6 \right. \\ &\quad \left. \pm (\mu_p - \mu_n - 1) C_{2v} \sum_{k=1}^{N_v} \tilde{b}_{v(k)} m_{v(k)}^6 \right] = \\ &= -\frac{64M_N^6}{2t^3 \ln^{p_2} |t|/\Lambda^2} [(\mu_p + \mu_n - 1) C_{2s} \kappa_{2s} \\ &\quad \pm (\mu_p - \mu_n - 1) C_{2v} \kappa_{2v}]. \end{aligned} \quad (9)$$

Here we introduced four dimensionless parameters $\kappa_{js,v}$ ($j = 1, 2$)

$$\begin{aligned} \kappa_{1s,v} &= \frac{1}{16M_N^4} \sum_{k=1}^{N_{s,v}} \tilde{a}_{s,v(k)} m_{s,v(k)}^4, \\ \kappa_{2s,v} &= \frac{1}{64M_N^6} \sum_{k=1}^{N_{s,v}} \tilde{b}_{s,v(k)} m_{s,v(k)}^6. \end{aligned} \quad (10)$$

Matching (9) with (3) yields the constants $C_{js,v}$

$$C_{1s,v} = -\frac{C_{1p} \pm C_{1n}}{\kappa_{1s,v}}, \quad C_{2s,v} = -\frac{C_{2p} \pm C_{2n}}{\kappa_{2s,v} (\mu_p \pm \mu_n - 1)} \quad (11)$$

Now, that the asymptotics (8) for the logarithmic functions are known, one could try to interpolate them in the whole range of t (A similar approach is used, for example, in Ref.[12].) As it shown by our numerical experiments, a good agreement with the data can be achieved by making use of the following interpolation formulas:

$$\begin{aligned} q_{s,v}(t) &= (1 + h_{1s,v} \ln \tilde{t} + g_{1s,v} \ln^2 \tilde{t})^{-p_1/2}, \\ \mu_{s,v}(t) &= (1 + h_{2s,v} \ln \tilde{t} + g_{2s,v} \ln^2 \tilde{t})^{-p_2/2}, \end{aligned} \quad (12)$$

where $\tilde{t} = 1 + |t|/\Lambda^2$. Parameters $h_{js,v}$ are free fit phenomenological parameters, which correspond to the sub-leading logarithms in pQCD. Parameters

$$g_{js,v} = (C_{js,v})^{-2/p_j} \quad (13)$$

correspond to the leading pQCD logarithms and are expressed according to Eq. (13) via the other fit parameters and constants $C_{1p,n}$, $C_{2p,n}$, which physically describe the partonic structure of the nucleon. These constants can, in principle, be calculated within pQCD or determined experimentally. If the numerical values of these constants were reliably known, parameters $g_{js,v}$ could be calculated via other fit parameters $\kappa_{js,v}$. To date, however, the multipliers in the partonic distribution functions, on which these constants depend, are not yet established, their values in different references vary within a certain ranges. So, the values $C_{1p,n}$, $C_{2p,n}$ are not unambiguously determined. In this situation we use $g_{js,v}$ as free fit parameters. Obtained in this way, these constants must be in agreement with pQCD estimations.

Thus, in the model presented here, all the parameters introduced except $h_{js,v}$ ($j=1,2$) have a direct physical meaning. The four adjusting parameters $h_{js,v}$ are necessary to tie together the low- and high Q^2 regions.

2.4 Vector Dominance model as a simple realization of the multipole expansion

In the vector dominance model the poles of the multipole expansion in t -plane are preset by the masses of vector mesons ρ , ω , ϕ . The numbers of poles, N_v and N_s , are the number of isovector (ρ) and isoscalar (ω , ϕ) mesons, respectively. In most of the earlier papers only three ground states of vector mesons, $\rho(770)$, $\omega(782)$ and $\phi(1020)$, are taken into account; in some models [15,16] $\rho(1450)$ state is also included.

Experimentally five $\rho\omega\phi$ -families are known. The three lightest of them are:

$$\begin{array}{lll} \rho(770), & \omega(782), & \phi(1019), \\ \rho(1450), & \omega(1420), & \phi(1680), \\ \rho(1700), & \omega(1650), & X(1750). \end{array} \quad (14)$$

One could argue, that the photon hadronization mainly proceeds through the vector mesons of the first family and the hadronization amplitudes $A(\gamma^* \rightarrow V_k^*)$ are small for the other families. This is indeed well known and follows from the experimental data on the widths $\Gamma(V \rightarrow e^-e^+) \sim |A(V \rightarrow \gamma^*)|^2$. In the multipole form factors, however, each coefficient of the multipole expansions is proportional to the hadronization amplitude multiplied on the amplitude $A(V_k^*N \rightarrow N)$ of the virtual vector meson absorption by the target nucleon. We define the composite amplitude as

$$A_k(eN \rightarrow eN) \sim A(\gamma^* \rightarrow V_k^*) \times A(V_k^*N \rightarrow N). \quad (15)$$

There is no reason to assume the composite amplitude, $A_k(eN \rightarrow eN)$, to be small, because the small hadronization amplitude could be multiplied on large absorption amplitude. Thus, the composite amplitudes could be comparable for all families. Matching the theoretical model with the experimental data, we will be able to fit the coefficients of the multipole expansion and thus extract information on the composite amplitudes.

The SR (6) are formulated for the sum of several multipole coefficients, that is for the whole meson spectrum. For the coefficients $b_{v,s(k)}$ there are three independent SR, which can be satisfied with at least three vector mesons of each type (isovector and isoscalar). Because of these SR, the number of free fit parameters in the model considered can be fewer, than that in the models with truncated spectrum, despite a larger number of mesons.

Another contribution to the nucleon form factors may come from light meson continua. This topic was recently investigated by the Mainz-Bonn-Julich group in Ref.[21, 33,34,35]. Within their model with only two-pion continuum [33], they obtained a good description of the data with the exception of the JLab G_{Ep}/G_{Mp} data. This is resolved in the following paper [35], where $\pi\pi$, $\rho\pi$ and

$K\bar{K}$ contributions are included. As it will be shown in Section 4, in the simplest modification of our model with meson poles only, we reach a similar or even a better level of accuracy for the overall fit. Since the continua give a main contribution at low Q^2 , while our main purpose was to describe all the data and to resolve the discrepancy at high Q^2 , we decided not to complicate our model and leave this topic beyond the scope of our paper. The price for keeping the model simple is its non-sensitivity to the physical effects that are important at low- Q^2 . In particular, beyond the scope of the model remains discussion on the role of sea quarks in the nucleon and on nucleon radii. Subsequent development of the model by including the meson continua can be a subject of further investigation.

Another non-trivial intriguing questions, widely discussed in QCD, are the nucleon spin structure [36,37] and nucleon strangeness [38,39,40]. DIS experiments show us, that quarks carry only a small fraction of the total angular momentum of the proton and strange sea quarks in the proton are strongly polarized opposite to the polarization of the proton. The challenge to understand this nontrivial structure of the proton requires studying the contributions from sea quarks, that is from the meson cloud. The complicated structure of the nucleon should somehow reveal itself also in elastic scattering. It would be reasonable to pose a problem to include these effects in the phenomenological model for elastic scattering. For these one would need to formulate the phenomenological model for the elastic spin structure functions, to introduce elastic strange form factors and also to consider meson cloud contributions. Such a model would contain a large number of free fit parameters, and thus would require more precise experimental data to fit them.

3 Soft photons

Let us proceed with the puzzling discrepancy between the Rosenbluth and polarization transfer experiments on a proton target. It was found recently, that the two-photon effects calculated within perturbation theory appear to be too small to explain the observed discrepancy [41,29]. In this situation we propose to search for the effects beyond the perturbation theory, that is to consider the soft bremsstrahlung accompanying the scattering of the charged particles. Notice, that by "soft bremsstrahlung" we refer here to quasiclassical non-perturbative effect. It should be distinguished from the far more known perturbative contribution, the infrared divergency of which cancels the correspondent divergency of the two-photon exchange.

The multiple emission of soft photons in the electron-nucleon scattering is a quasi-classical process with a peculiar features due to internal nucleon structure. The incoming electron scatters in a compound field, originated from the nucleon charge (Dirac form factor) and its magnetic moment (Pauli form factor). It was noticed in [30], that the soft photons are mainly produced in the electric field of the Dirac form factor, while the contribution of Pauli form factor is negligible. This disparity of the two form factors can be also shown by direct calculation of

the spectral distribution and the total intensity of the soft bremsstrahlung. This calculation is done in Section 3.1 relying on the calculation method from [42, Problem 1 to §98]. This calculation shows, that two non-interfering fluxes of photons, "electric" and "magnetic" ones, have different spectral functions and different average number of photons. On this grounds we suppose, the soft photon emission beyond the perturbation theory can be taken into account by multiplying the Dirac and Pauli form factors on the corresponding "electric" and "magnetic" emission amplitudes. The corresponding calculations are done in Section 3.2.

In the case of Rosenbluth type experiments, where protons in the final state are not polarized, multiple emission of soft photons is natural and the emission amplitudes are characterised by the average numbers of "electric" and "magnetic" photons. In the polarisation transfer experiments, however, any emitted photon would carry away the angular momentum and thus prevent the transfer of polarization, which would destroy the correlation of the electron and proton polarization vectors. Thus we assume, that in the polarization transfer experiments no soft photon can be emitted.

In Sections 3.3, 3.4 and 3.5 we show that within our model the difference with respect to the multiple emission of the soft photons can be responsible for the observed discrepancy and ensures that the form factors, observed in the beam-target asymmetry experiments are different from those in both the Rosenbluth and polarization transfer experiments.

3.1 Dirac and Pauli subsystems in the multiple emission of soft photons

Let us consider the differential cross section of eN scattering at the angle θ with the emission of one photon of frequency ω :

$$d\sigma = \alpha_{\text{em}} \frac{d\omega}{\omega} F(\xi(\theta)) d\sigma_{\text{Ros}}(\theta). \quad (16)$$

The amplitude $F(\xi(\theta))$ of soft photon emission

$$F(\xi) = \frac{2}{\pi} \left[\frac{2\xi^2 + 1}{\xi\sqrt{\xi^2 + 1}} \ln(\xi + \sqrt{\xi^2 + 1}) - 1 \right],$$

$$\xi = \frac{\varepsilon}{m} \sin \frac{\theta}{2}$$

was calculated in [42, §98] within perturbation theory and describes the emission a soft photon integrated over the whole range of photon angles. Here ε , and m are correspondingly electron energy and mass.

In one-photon approximation it was shown, that the ultrarelativistic electrons are mainly emitted within the angle range

$$\frac{m^2\omega}{\varepsilon^3} \ll \theta \lesssim \frac{m}{\varepsilon}. \quad (17)$$

For a nucleon with charge Z and anomalous magnetic moment μ_{an} , the elastic cross section for such small angles

is

$$d\sigma_{\text{Ros}} \approx \frac{4\alpha^2}{\varepsilon^2\theta^4} \left(F_1^2(t) - \frac{t}{4M_N^2} F_2^2(t) \right) d\Omega$$

$$\approx 4\alpha^2 \left(\frac{Z^2}{\varepsilon^2\theta^4} + \frac{\mu_{an}^2}{4M_N^2\theta^2} \right). \quad (18)$$

The spectral distribution of the soft emission can be obtained by substituting (18) into (16) and integrating over the electron scattering angles. Keeping in mind, that in the region of angles (17) one has $\xi \ll 1$ and $F(\xi) \approx (8/3\pi)\xi^2$, one gets:

$$d\sigma_\omega = \frac{16\alpha^3}{3m^2} \frac{d\omega}{\omega} \int_{\theta_{\min}(\omega)}^{\theta_{\max}} \left(\frac{Z^2}{\theta} + \frac{\mu_{an}^2 \varepsilon^2}{4M_N^2} \theta \right) d\theta =$$

$$= d\sigma_\omega^{(Z)} + d\sigma_\omega^{(\mu_{an})},$$

$$d\sigma_\omega^{(Z)} = \frac{16Z^2\alpha^3}{3m^2} \ln \frac{\varepsilon^2}{m\omega} \frac{d\omega}{\omega},$$

$$d\sigma_\omega^{(\mu_{an})} = \frac{2\alpha^3\mu_{an}^2}{3M_N^2} \frac{d\omega}{\omega}. \quad (19)$$

According to Eq. (19) soft emission on the proton consist of two subsystems with different intensities and different spectral distributions. The term $d\sigma_\omega^{(Z)}$ describes the electric dipole emission, generated in the field of the Dirac form factor; the term $d\sigma_\omega^{(\mu_{an})}$ describes the magnetic bremsstrahlung in the field of the Pauli form factor. As we have already mentioned, the magnetic bremsstrahlung is strongly suppressed in comparison with the dipole emission:

$$\frac{d\sigma_\omega^{(Z)}}{d\sigma_\omega^{(\mu_{an})}} = \frac{8Z^2M_N^2}{\mu_{an}^2m^2} \ln \frac{\varepsilon^2}{m\omega} \gg 1. \quad (20)$$

However, as a matter of principle, each type of emission is experimentally verifiable. Indeed, for the target neutron ($Z = 0$) only magnetic bremsstrahlung is possible and its characteristics coincide with those for the proton up to a multiplier. Thus, having neutron data, one could differentiate the two subsystems of the soft emission for the proton. Notice also, that the soft photons from different subsystems have different characteristic frequency spacing. This fact can be proved by analyzing the total cross section of the bremsstrahlung $\sigma_\gamma = \int d\sigma_\omega$, which can be obtained by integrating (19) over the photon frequencies. The result of integration, as it is conventional in the soft photon theory, depends on two parameters: the minimal ω_{\min} and maximal ω_{\max} frequencies of the soft emission:

$$\begin{aligned}\sigma_\gamma &= \sigma_\gamma^{(Z)} + \sigma_\gamma^{(\mu_{an})}, \\ \sigma_\gamma^{(Z)} &= \frac{16Z^2\alpha^3}{3m^2} \left(2\ln\frac{\varepsilon}{m} \ln\frac{\omega_{max}(Z)}{\omega_{min}} - \frac{1}{2}\ln^2\frac{\omega_{max}(Z)}{m} + \frac{1}{2}\ln^2\frac{\omega_{min}}{m} \right), \\ \sigma_\gamma^{(\mu_{an})} &= \frac{2\alpha^3\mu_{an}^2}{3M_N^2} \ln\frac{\omega_{max}(\mu_{an})}{\omega_{min}}.\end{aligned}\quad (21)$$

The minimal frequency, ω_{min} , is determined by the accuracy up to which the energies of the initial and final particles are measured by a given detector. The very notion about the soft photons is constrained by the approximate factorization of the scattering amplitude with one photon emission, which is valid only in the low-frequency region. Thus, the maximal frequencies, $\omega_{min}(Z, \mu_{an})$, inevitably appear in the soft photon phenomenology as a cut-off parameters governed by the conditions that the photons are soft. It follows from (21), that $\sigma_\gamma^{(\mu_{an})} < \sigma_\gamma^{(Z)}$.

Evidently the average numbers of the soft photons emitted in the field of the Pauli and Dirac form factors must satisfy the same inequality $\bar{n}^{(\mu_{an})} < \bar{n}^{(Z)}$. Besides, $\sigma_\gamma^{(\mu_{an})}$ is of logarithmic order, while $\sigma_\gamma^{(Z)}$ is of squared logarithmic order. It is natural to suppose, that the average number of photons have correspondingly the same orders of magnitude $\bar{n}^{(\mu_{an})} \sim \ln\omega$, $\bar{n}^{(Z)} \sim \ln^2\omega$.

When the general formula for the average number of the soft photons \bar{n} is derived in [42], § 120, it is shown that the information about the field, in which the soft emission is formed, reveals only in the cut-off parameter ω_{max} . The approximate formula accurate to the logarithm squared is given at the end of § 120 in [42]:

$$\bar{n} \simeq \frac{\alpha}{2\pi} \left[\ln^2\frac{|t|}{m^2} + 2\ln\frac{|t|}{m^2} \left(\ln\frac{\omega_{max}^2}{\omega_{min}^2} - \ln\frac{\varepsilon^2}{m^2} \right) \right]. \quad (22)$$

A more accurate expression is obtained recently in [24]. Since the average number of photons emitted in the field of the Dirac form factor is determined with double logarithmic accuracy, the estimate for $\bar{n}_{(Z)} \equiv \bar{n}_{1p}$ can be obtained from (22) with $\omega_{max}(Z) \sim \varepsilon$:

$$\bar{n}_{1p} \simeq \frac{\alpha}{2\pi} \ln^2\frac{|t|}{\omega_{min}^2}. \quad (23)$$

Further for numerical calculations, it will be convenient to modify this formula and make it regular at $|t| = 0$. We will use

$$\bar{n}_{1p} \simeq \frac{\alpha}{2\pi} \ln^2\left(1 + \frac{|t|}{\Lambda_\gamma^2}\right). \quad (24)$$

Within the double logarithmic accuracy, Λ_γ preserve its meaning as a minimal frequency of the soft emission.

When estimating the average number of magnetic-bremsstrahlung photons $\bar{n}_{(\mu_{an})} \equiv \bar{n}_{2N}$, the cut-off parameter $\omega_{max}(\mu_{an})$ must be chosen in such a way that the expression (22) turns into logarithm (the squares of

the logarithms must be cancelled). This is achieved with $\omega_{max}(\mu_{an}) \sim \sqrt{m\varepsilon}$:

$$\bar{n}_{2N} \simeq \frac{\kappa\alpha}{2\pi} \ln\frac{|t|}{m^2}, \quad \kappa = \ln\frac{m^2\sqrt{|t|}}{\omega_{min}^2\varepsilon}. \quad (25)$$

Thus, for $\omega_{max}(\mu_{an}) \sim \sqrt{m\varepsilon}$ parameter κ is not logarithmically large, so the estimate (25) is in agreement with the expression for $\sigma_\gamma^{(\mu_{an})}$, given in (21). Of course, the contribution to κ is also given by sub-leading logarithmic terms, which are not present in (22) and can be found only in more accurate calculations. Further on, however, the only fact important for our consideration is that the average number of electric-dipole soft photons considerably exceeds that of magnetic-bremsstrahlung ones.

$$\bar{n}_{2n} \sim \bar{n}_{2p} \ll \bar{n}_{1p}, \quad (26)$$

3.2 How soft photon emission can modify observables

Thus, beyond perturbation theory, the Dirac and Pauli form factors are disparate, which is revealed in Eqs. (20), (26). Therefore, *nonperturbative* probability of soft emission cannot be represented as a single multiplier outside the pure elastic Rosenbluth cross section. Since the process under discussion is classic, the soft emission depends not only on the initial and final electron states, but also on the peculiar characteristics of the quasiclassical trajectory. The multiple emission of soft photons at the alteration of electron trajectory proceeds during the period of time τ that is significantly longer than the inverse characteristic photon frequency, $\omega\tau \gg 1$. In this situation, contrary to the one-photon approximation, allowance must be made for the soft emission over large angles. The electron trajectory is formed by the superposition of the electromagnetic fields, generated individually by the Dirac and Pauli form factors, which leads to the two distinct subsystems of the soft photon emission.

On the basis of the above qualitative considerations, we put forward the idea, that the Dirac and Pauli scattering amplitudes with emission of n photons differ from the corresponding elastic amplitudes and can be obtained by multiplying those on the two different *nonperturbative* amplitudes of n soft photon emission $A_{1N}(n)$, $A_{2N}(n)$. Modification of the scattering amplitudes leads to the modification of the form factors:

$$F_{1N}^{(n\gamma)} = A_{1N}(n)F_{1N}, \quad F_{2N}^{(n\gamma)} = A_{2N}(n)F_{2N}.$$

As we discussed earlier, in the polarization transfer experiments only events without real photon emission ($n = 0$) can contribute. In Rothenbluth experiments, on the contrary, the processes with emission of any number n of soft photons occur. Thus the *nonperturbative* amplitudes of the soft photon emission are different for these two experiments.

About the photon emission amplitudes $A_{1N}(n)$, $A_{2N}(n)$ it is known, that their averaged squares are equal to the

corresponding probabilities calculated via the Poisson distributions:

$$\langle |A_{1N}(n)|^2 \rangle = w_{1N}(n) = \frac{\bar{n}_{1N}^n}{n!} e^{-\bar{n}_{1N}}, \quad (27)$$

$$\langle |A_{2N}(n)|^2 \rangle = w_{2N}(n) = \frac{\bar{n}_{2N}^n}{n!} e^{-\bar{n}_{2N}}. \quad (28)$$

The averaged numbers of the "dipole" type \bar{n}_{1N} and "magnetic-bremsstrahlung" type \bar{n}_{2N} photons are different and as well depend on the nucleon, in the field of which the emission is formed (target nucleon in our case). For the target proton, photon emission in the short-range Pauli field is negligible in comparison with that in the long-range Dirac field, $\bar{n}_{2p} \ll \bar{n}_{1p}$, \bar{n}_{1p} will be give below in Eq.(24). For the neutron target, $\bar{n}_{1n} \ll \bar{n}_{1p}$ because the Dirac form factor is small, and $\bar{n}_{2n} \sim \bar{n}_{2p}$. For our purposes it would be enough to estimate

$$A_{1n}(0) \simeq A_{2n}(0) \simeq 1, \quad A_{1n}(n) \simeq A_{2n}(n) \simeq 0 \text{ for } n \geq 1,$$

Within this assumption, the electric and magnetic form factors of neutron are not modified by the soft photon emission and are given by the standard expressions

$$\begin{aligned} G_{En}(t) &= F_{1n}(t) + \frac{t}{4M_N^2} F_{2n}(t), \\ G_{Mn}(t) &= F_{1n}(t) + F_{2n}(t), \end{aligned} \quad (29)$$

So, our model predict that the ratio of the neutron form factors, obtained in different types of experiments must be approximately the same.

3.3 Form factors from Rosenbluth scattering

To obtain the proton form factors, let us separate from the Rosenbluth formula the combination of the form factors $\sigma_{ext}(t, \theta)$ which enters the differential cross section

$$\begin{aligned} \frac{d\sigma_{Ros}}{d\Omega} &= f_{rec} \sigma_{Mott} \sigma_{ext}(t, \theta), \\ \sigma_{ext}(t, \theta) &= \frac{\left[G_{Ep}^{(Ros)} \right]^2 - \frac{t}{4M_N^2} \left[G_{Mp}^{(Ros)} \right]^2}{1 - \frac{t}{4M_N^2} - \frac{t}{2M_N^2} \left[G_{Mp}^{(Ros)} \right]^2 \tan^2 \frac{\theta}{2}}. \end{aligned} \quad (30)$$

The squares of the form factors are calculated as

$$\begin{aligned} \left[G_{Ep}^{(Ros)} \right]^2 &= \sum_{n=0}^{\infty} \left\langle \left[A_{1p}(n) F_{1p} + \frac{t}{4M_N^2} A_{2p}(n) F_{2p} \right]^2 \right\rangle = \\ &= \left[F_{1p} + \frac{t}{4M_N^2} F_{2p} \right]^2 \\ &\quad - \left[1 - \sum_{n=0}^{\infty} \langle A_{1p}(n) A_{2p}(n) \rangle \right] \frac{t}{2M_N^2} F_{1p} F_{2p}, \\ \left[G_{Mp}^{(Ros)} \right]^2 &= \sum_{n=0}^{\infty} \langle [A_{1p}(n) F_{1p} + A_{2p}(n) F_{2p}]^2 \rangle = \\ &= [F_{1p} + F_{2p}]^2 - 2 \left[1 - \sum_{n=0}^{\infty} \langle A_{1p}(n) A_{2p}(n) \rangle \right] F_{1p} F_{2p}. \end{aligned} \quad (31)$$

In Eqs.(31) there is an interference term of Dirac and Pauli form factors, that is interference of the soft emission of different types. In the first summand of Eq. (30), which gives the dominant contribution to the scattering through small angles, the two interference terms cancel out. Therefore the interference effects would be noticeable only at large scattering angles.

At large t the experimental procedure includes two steps. At the first step the coefficient before the $\tan^2(\theta/2)$ is measured and magnetic form factor $G_{Mp}^{(Ros)}(t)$ is deduced. Having it known and provided that the accuracy of the measurement is high enough, the electric form factor $G_{Ep}^{(Ros)}(t)$ is extracted. According to this procedure, the experimentally observed values are described by Eqs. (31), which including interference terms.

The averaged interference terms in the two special cases are

$$\begin{aligned} \sum_{n=0}^{\infty} \langle A_{1p}(n) A_{2p}(n) \rangle &= 1 \quad \text{if} \quad 1) \bar{n}_{1p} = 0, \bar{n}_{2p} = 0; \\ &2) \bar{n}_{1p} = \bar{n}_{2p}. \end{aligned} \quad (32)$$

The properties (28), (32) can be satisfied by choosing the amplitudes in a very simple form

$$A_{1p}(n) = \sqrt{w_{1p}(n)} \quad A_{2p}(n) = \sqrt{w_{2p}(n)} \quad (33)$$

Substituting (33) into (31) yields expressions, which can be further simplified for $\bar{n}_{2p} \ll \bar{n}_{1p}$:

$$\begin{aligned}
\left[G_{Ep}^{(Ros)}\right]^2 &= \left[F_{1p} + \frac{t}{4M_N^2} F_{2p}\right]^2 \\
&- \left[1 - e^{-(\sqrt{\bar{n}_{1p}} - \sqrt{\bar{n}_{2p}})^2/2}\right] \frac{t}{2M_N^2} F_{1p} F_{2p} \simeq \\
&\simeq \left[F_{1p} + \frac{t}{4M_N^2} F_{2p}\right]^2 - \left(1 - e^{-\bar{n}_{1p}/2}\right) \frac{t}{2M_N^2} F_{1p} F_{2p}, \\
\left[G_{Mp}^{(Ros)}\right]^2 &= [F_{1p} + F_{2p}]^2 \\
&- 2 \left[1 - e^{-(\sqrt{\bar{n}_{1p}} - \sqrt{\bar{n}_{2p}})^2/2}\right] F_{1p} F_{2p} \simeq \\
&\simeq [F_{1p} + F_{2p}]^2 - 2 \left(1 - e^{-\bar{n}_{1p}/2}\right) F_{1p} F_{2p}.
\end{aligned} \tag{34}$$

$$R_p^{(Ros)} = \sqrt{\frac{\left[G_{Ep}^{(Ros)}\right]^2}{\left[G_{Mp}^{(Ros)}\right]^2}} \tag{35}$$

The average number of soft photons is given in Eq. (24). When fitting the experimental data, the minimal frequency A_γ of the soft emission, according to its physical status, is considered as a free fit parameter.

As one could see the asymmetry in the soft photon emission by Dirac and Pauli form factors considerably modifies (with respect to naive expectations) the relations between the theoretically calculated $F_{1,2p}$ and experimentally measured $G_{E,Mp}^{(Ros)}$ quantities. One should however remember, that this formulas are only applicable to the Rosenbluth extraction.

3.4 Form factors from recoil polarization experiments

In elastic scattering of polarized electrons from a nucleon, the nucleon is transferred a polarization, whose components along (P_l) and perpendicular to (P_t) the nucleon momentum are proportional to G_M^2 and $G_E G_M$, respectively. Such polarization transfer can only proceed without the soft photon emission. Thus, the Dirac form factor is multiplied by the probability amplitude with zero photons $A_{1p}(0) = e^{-\bar{n}_{1p}/2}$ (only one nonzero term remains in the whole sum). The modification of Pauli form factor is negligible (within the accuracy of our consideration).

As a result, the experimentally measured ratio $P_t/P_l \sim G_E G_M / G_M^2 = G_E / G_M$ is proportional to the ratio of the form factors, which can be calculated as

$$R_p^{(pol)} \equiv \frac{\mu_p G_{Ep}^{(pol)}}{G_{Mp}^{(pol)}} = \frac{\mu_p \left(e^{-\bar{n}_{1p}/2} F_{1p} + \frac{t}{4M_N^2} F_{2p} \right)}{e^{-\bar{n}_{1p}/2} F_{1p} + F_{2p}}. \tag{36}$$

with the Dirac and Pauli form factors, defined differently from the naive expectation as well as from (35).

3.5 Form factors from beam-target asymmetry

Another type of experiments is scattering of a polarized electron against a polarized target nucleon. With the target polarization axis in the scattering plane and perpendicular to the momentum transfer \mathbf{q} , the asymmetry A_{TL} (the difference of the cross sections for opposite electron beam helicities) is proportional to $G_E G_M$. With the target polarization axis in the scattering plane and parallel to \mathbf{q} , the asymmetry A_T is proportional to G_M^2 . Experimentally measured is the ratio:

$$\frac{A_{TL}}{A_T} \sim \frac{G_E G_M}{G_M^2}. \tag{37}$$

In such experiments the final state is inclusive, so the soft photon emission is possible, like in Rosenbluth scattering. The value $G_E G_M$ must be calculated as follows

$$\begin{aligned}
[G_{Ep} G_{Mp}]^{(bta)} &= \sum_{n=0}^{\infty} \langle [A_{1p}(n) F_{1p} + A_{2p}(n) F_{2p}] \times \\
&\times \left[A_{1p}(n) F_{1p} + \frac{t}{4M_N^2} A_{2p}(n) F_{2p} \right] \rangle = \\
&= \left[F_{1p} + \frac{t}{4M_N^2} A_{2p}(n) F_{2p} \right] [F_{1p} + F_{2p}] \\
&- \left(1 - e^{-\bar{n}_{1p}/2}\right) F_{1p} F_{2p},
\end{aligned} \tag{38}$$

and G_M^2 is the same as in the Rosenbluth experiments $[G_{Mp}^2]^{bta} = [G_{Mp}^2]^{Ros}$. So, the ratio of the form factors

$$R_p^{(bta)} \equiv \frac{\mu_p [G_{Ep} G_{Mp}]^{(bta)}}{[G_{Mp}^2]^{(bta)}} \tag{39}$$

is defined differently from (36) as well as from (35).

3.6 Recap

Let us shortly summarize the results of this section. To interpret experimental data from different kinds of experiments, different expressions for the form factors must be used. All the data can be physically and mathematically described with the same theoretically defined form factors $F_{1,2p}$ (7) and the same average number of soft electric-dipole photons \bar{n}_{1p} . The electric and magnetic form factors and their ratios are given, however, by different expressions: Eq. (34) for Rosenbluth separation technique, Eq. (36) for polarization transfer, and Eq. (39) for beam-target asymmetry experiments.

4 Fit of the experimental data

The model described in previous sections is used to fit all experimental data on the form factors (with the references summarized in Tables 1,2) available to date. In the framework of this model the form factors $F_{1,2}^{p,n}$ are

Table 1. Data on proton form factors.

Measurement	Q^2 -range	reference
G_{Ep}		
$p(e, e')$	0.01 - 0.05	Simon et al. [44]
	0.04 - 1.75	Price et al. [45]
	0.39 - 1.95	Berger et al. [46]
	1.00 - 3.00	Walker et al. [47]
	1.75 - 8.83	Andivahis et al. [48]
$p(e, p')$	2.64 - 4.10	Qattan et al. [49]
	0.65 - 5.2	Christy et al. [50]
$d(e, e'p)$	0.27 - 1.76	Hanson et al [51]
G_{Mp}		
$p(e, e')$	0.02 - 0.15	Hoehler et al. [52]
	0.16 - 0.86	Janssens et al. [53]
	0.39 - 1.75	Berger et al. [46]
	0.67 - 3.00	Bartel et al. [54]
	1.00 - 3.00	Walker et al. [47]
	1.50 - 3.75	Litt et al. [55]
	1.75 - 7.00	Andivahis et al. [48]
	2.86 - 31.2	Sill et al. [56]
$d(e, e'p)$	0.27 - 1.76	Hanson et al [51]
G_{Ep}/G_{Mp}		
$p(\vec{e}, e' \vec{p})$	0.37 - 0.44	Pospischil et al. [57]
	0.38 - 0.50	Milbrath et al. [58]
	0.40	Dieterich et al. [59]
	0.49 - 3.47	Jones et al. [60]
	1.13	Mac Lachlan et al. [61]
	3.50 - 5.54	Gayou et al. [62, 8]
$\vec{p}(\vec{e}, e'p)$	0.15 - 0.65	Crawford et al. [63]
$\vec{p}(\vec{e}, e'p)$	1.51	Jones et al. [64]

Table 2. Data on neutron form factors.

Measurement	Q^2 -range	reference
G_{En}		
$\vec{d}(\vec{e}, e'n)p$	0.21	Passchier et al. [65]
	0.50	Zhu et al. [66]
$\vec{^3He}(\vec{e}, e'n)$	0.40	Becker et al. [67, 68, 69]
$d(\vec{e}, e' \vec{n})p$	0.5, 1.0	Warren et al. [70, 71]
	0.67	Rohe et al. [72]
	0.67	Bermuth et al. [73]
?		Schiavilla et al. [74]
$d(e, e')$	0.27 - 1.76	Hanson et al [51]
	1.75 - 4.00	Lung et al. [75]
G_{Mn}		
$d(e, e'n)p$	0.07 - 0.89	Kubon et al. [76]
	0.11	Anklin et al. [77]
	0.11 - 0.26	Markowitz et al. [78]
	0.13 - 0.61	Bruins et al. [79]
	0.24 - 0.78	Anklin et al. [80]
$d(e, e'p)$	0.27 - 1.76	Hanson et al [51]
$\vec{^3He}(\vec{e}, e'n)$	0.10, 0.20	Xu et al. [81, 69]
	0.19	Gao et al. [82]
	0.3 - 0.6	Xu et al. [83]
$d(e, e')$	1.75 - 4.00	Lung et al. [75]
	2.50 - 10.0	Rock et al. [84]
G_{En}/G_{Mn}		
$d(\vec{e}, e' \vec{n})p$	0.30 - 0.8	Glazier et al. [85]
	0.15	Herberg et al. [86]
	0.26	Eden et al. [87]
	0.34	Ostrick et al. [88]
	0.49 - 1.47	Madey et al.[89, 90, 91]

described by Eqs. (7) with the four phenomenological logarithmic functions $q_{s,v}$, $\mu_{s,v}$ given in (12). The pole positions $m_{\rho, \omega, \phi}$ were taken as masses of vector mesons from PDG[43]. Parameters p_1 , p_2 in these functions are calculated according to (3) with the effective number of quark flavors being given by interpolation formula

$$n_f = 2 + \frac{|t|}{|t| + 4m_s^2} + \frac{|t|}{|t| + 4m_c^2}, \quad (40)$$

where $m_s \approx 0.15$ GeV and $m_c \approx 1.5$ GeV are masses of strange and charmed quarks correspondingly. The form factors in Rosenbluth experiments and the ratio in polarization experiments are determined in Eqs. (34), (36) with the averaged number of the emitted soft photons from (24).

In the model under consideration the coefficients of the multipole expansions obey the SR (6) and, thus, not all of them are free fit parameters. In the isovector sector from N_v parameters $\tilde{a}_{v(k)}$, which satisfy two SR, and N_v

parameters $\tilde{b}_{v(k)}$, which satisfy three SR, $2N_v - 5$ parameters are independent. In the isoscalar sector one ends up analogically with $2N_s - 5$ independent free parameters.

The model contains 10 more parameters: 9 in the logarithmic functions (12) and 1 in Eq. (24) for the average number of soft photons. The status of $g_{1,2s,v}$ and $h_{1,2(s,v)}$ was discussed in subsection 2.3, Λ approximately equals the QCD scale and Λ_γ is a minimal frequency of soft photon emission.

As we have already mentioned, to satisfy three of the introduced SR, at least three vector meson families are to be considered. Below we describe the fit obtained in the framework of the simplest modification of our model with $N_v = 3$ and the isovector poles identified with the squared ρ -meson masses. In this model all the three parameters $\tilde{b}_{v(k)} \equiv \tilde{b}_{\rho(k)}$ are fixed by the SR and not fitted. Three parameters $\tilde{a}_{v(k)} \equiv \tilde{a}_{\rho(k)}$ satisfy two SR, so only one of them is independent. It is chosen as κ_{1v} , introduced in (10).

In this simplest modification only three ω mesons are taken into account in the isoscalar sector and ϕ -mesons are neglected. Such simplification is physically justified because the eN interaction through the ϕ mesons contributes only little to the structure of the form factors. Indeed, for the ideal singlet-octet mixing the ϕ mesons consist of two strange quarks $\phi = \bar{s}s$, and thus interact only with the virtual strange component of the nucleon, which is insignificant for the nucleon structure. Deviations from the ideal mixing are suppressed by small parameters. To the zeroth order on these parameters, interactions of ϕ mesons with ud - component of the nucleon are negligible. After excluding ϕ mesons from the isoscalar sector of the model, parameters $\tilde{b}_{s(k)} = \tilde{b}_{\omega(k)}$ are fixed by the three SR and among three parameters $\tilde{a}_{s(k)} = \tilde{a}_{\omega(k)}$ only one is independent. It is chosen as κ_{1s} from Eq. (10).

This simplest modification of the model without ϕ mesons is used for the preliminary joined fit of the Rosenbluth and polarization data. There are 12 fit parameters common for the 5 sets of data. The result of the fit is shown in Figs. 1–4, the accuracy of the fit being $\chi^2/dof = 0.86$. The parameters of the model, obtained in our fit are:

$$\begin{aligned} \kappa_{1v} &= -0.896, & \kappa_{1s} &= -0.0814, \\ g_{1v} &= 0.0949, & h_{1v} &= 0, \\ g_{1s} &= 0.0138, & h_{1s} &= 0, \\ g_{2v} &= 0.326, & h_{2v} &= -0.118, \\ g_{2s} &= 0.0813, & h_{2s} &= -0.568 \\ \Lambda &= 0.163 \text{ GeV}, & \Lambda_\gamma &= 0.00405 \text{ GeV} \end{aligned} \quad (41)$$

The errors are hard to estimate due to nonlinearity of the problem.

An attempt to improve this fit by including ϕ -mesons (of all the three generations considered here) leads to a better accuracy of the fit, $\chi^2/dof = 0.81$. Keeping in mind, however, that there are additional 6 fit parameters for this case (three \tilde{a}_s and three \tilde{b}_s), this improvement of accuracy does not look significant. In any case, the difference between the curves for the cases with and without ϕ -mesons is hardly noticeable. For this reason we prefer to leave the detailed discussion of the ϕ -meson contribution for further investigation.

5 Predictions

In this section we shortly summarize the predictions of our model, which in principle can be tested experimentally.

1. For proton the formulas for experimentally measured electric and magnetic form factors and their ratios are different for Rosenbluth (see Eq. (34), (35)), polarization (see Eqs. (36)) and beam-target asymmetry (see Eq. (39)) experiments. The ratios are shown in Fig. 2. They satisfy the inequality

$$R^{(pol)}(Q^2) < R^{(bta)}(Q^2) < R^{(Ros)}(Q^2)$$

2. Rothenbluth electric form factor of the proton does not goes to zero, the ratio of the form factors grows with increasing Q^2 . The ratio, measured in the polarization

transfer experiments, crosses zero at $Q^2 \sim 9-10 \text{ GeV}^2$. The ratio, measured in the beam-target asymmetry experiments, crosses zero at $Q^2 \sim 17-19 \text{ GeV}^2$

3. For neutron the data from all three types of experiments coincide:

$$G_{En}^{(Ros)} = G_{En}^{(pol)} = G_{En}^{(bta)} = G_{En}$$

$$G_{Mn}^{(Ros)} = G_{Mn}^{(pol)} = G_{Mn}^{(bta)} = G_{Mn}$$

$$R_n^{(Ros)} = R_n^{(Ros)} = R_n^{(Ros)} = G_{En}/G_{Mn}$$

and are given by conventional formulas (29). The ratio of the form factors is shown in Fig. 4.

6 Conclusions

Thus, we propose an interpretation of the electromagnetic nucleon form factors on the basis of the following physical conceptions:

1. multipole structure of the form factors, which correspond to the vector meson dominance with taking into account at least three $\omega\rho\phi$ - families.
2. logarithmic dependencies of the coefficients of the multipole expansions reflect the renormalization of the nucleon-meson coupling constants by the quark-gluon effects at small distances;
3. Superconvergence Relations for the meson parameters ensures the agreement of the multipole form factors asymptotics the pQCD asymptotics; in this way we account for QCD effects at the level of valence quarks.
4. form factors, extracted from the cross sections, are modified by the effect of the soft emission, which is different for different experiments. This effect allows to resolve the discrepancy between the Rosenbluth and polarization measurements.

In the framework of this model the Dirac $F_{1p,n}$ and Pauli $F_{2p,n}$ form factors are the same for all types of experiments. They are obtained from the fit with the results

explicitly given in the following equations:

$$\begin{aligned}
 F_{1p,n} &= \frac{1}{2} [F_{1s} \pm F_{1v}], & F_{2p,n} &= \frac{1}{2} [F_{2s} \pm F_{2v}], \\
 F_{1s} &= \left[\frac{0.923}{0.612 + Q^2} + \frac{-1.314}{2.031 + Q^2} + \frac{0.391}{2.789 + Q^2} \right] \times \\
 &\quad \left[1 + 0.0138 \ln^2 \left(1 + \frac{Q^2}{0.0266} \right) \right]^{-p_1} \\
 F_{1v} &= \left[\frac{-0.793}{0.602 + Q^2} + \frac{16.018}{2.147 + Q^2} + \frac{-15.226}{2.958 + Q^2} \right] \times \\
 &\quad \left[1 + 0.0949 \ln^2 \left(1 + \frac{Q^2}{0.0266} \right) \right]^{-p_1} \\
 F_{2s} &= \left[\frac{-0.135}{0.612 + Q^2} + \frac{0.388}{2.031 + Q^2} + \frac{-0.253}{2.789 + Q^2} \right] \times \\
 &\quad \left[1 - 0.568 \ln \left(1 + \frac{Q^2}{0.0266} \right) + 0.0813 \ln^2 \left(1 + \frac{Q^2}{0.0266} \right) \right]^{-p_2} \\
 F_{2v} &= \left[\frac{3.893}{0.602 + Q^2} + \frac{-11.295}{2.147 + Q^2} + \frac{7.402}{2.958 + Q^2} \right] \times \\
 &\quad \left[1 - 0.118 \ln \left(1 + \frac{Q^2}{0.0266} \right) + 0.326 \ln^2 \left(1 + \frac{Q^2}{0.0266} \right) \right]^{-p_2} \\
 p_1 &= 2 + \frac{3.555}{11 - 0.67n_f}, & p_2 &= \frac{2.667}{11 - 0.67n_f}, \\
 n_f &= 2 + \frac{Q^2}{Q^2 + 0.0900} + \frac{Q^2}{Q^2 + 9.00}
 \end{aligned} \tag{42}$$

The experimentally measured form factors and their ratios are shown in Figs. 1, 2, 3, 4. They are given in Eqs. (29) for neutron and Eqs. (34), (35), (36) (39) for proton. They depend not only on Dirac and Pauli form factors, but also on the average number of the soft photons \bar{n}_{1p} , emitted in the field of the Dirac proton form factor in the experiments with inclusive final states

$$\bar{n}_{1p} = 0.116 \cdot 10^{-2} \ln^2 \left(1 + \frac{Q^2}{0.164 \cdot 10^{-4} \text{ GeV}^2} \right). \tag{43}$$

GV is grateful to the participants of the Theory Group Seminar in JINR, Dubna, where he had a pleasure to present his talk, for their comments and suggestions. Discussions with Prof. A. Efremov were especially helpful.

References

1. D. Day, Eur. Phys. J. **A31**, 560 (2007)
2. J. Friedrich, T. Walcher, Eur. Phys. J. **A17**, 607 (2003), [hep-ph/0303054](#)
3. E. Tomasi-Gustafsson, F. Lacroix, C. Duterte, G.I. Gakh, Eur. Phys. J. **A24**, 419 (2005), [nucl-th/0503001](#)
4. J. Arrington, Eur. Phys. J. **A17**, 311 (2003), [hep-ph/0209243](#)
5. A. Bodek, H. Budd, J. Arrington, AIP Conf. Proc. **698**, 148 (2004), [hep-ex/0309024](#)
6. H. Budd, A. Bodek, J. Arrington (2003), [hep-ex/0308005](#)
7. J.J. Kelly, Phys. Rev. **C70**, 068202 (2004)
8. V. Punjabi et al., Phys. Rev. **C71**, 055202 (2005), [nucl-ex/0501018](#)
9. S.J. Brodsky, G.R. Farrar, Phys. Rev. **D11**, 1309 (1975)
10. G.P. Lepage, S.J. Brodsky, Phys. Rev. **D22**, 2157 (1980)
11. A.V. Belitsky, X.d. Ji, F. Yuan, Phys. Rev. Lett. **91**, 092003 (2003), [hep-ph/0212351](#)
12. S.J. Brodsky, J.R. Hiller, D.S. Hwang, V.A. Karmanov, Phys. Rev. **D69**, 076001 (2004), [hep-ph/0311218](#)
13. M. Guidal, M.V. Polyakov, A.V. Radyushkin, M. Vanderhaeghen, Phys. Rev. **D72**, 054013 (2005), [hep-ph/0410251](#)
14. M.F. Gari, W. Kruempelmann, Phys. Rev. **D45**, 1817 (1992)
15. E.L. Lomon, Phys. Rev. **C64**, 035204 (2001), [nucl-th/0104039](#)
16. E.L. Lomon, Phys. Rev. **C66**, 045501 (2002), [nucl-th/0203081](#)
17. F. Iachello, Eur. Phys. J. **A19**, Suppl129 (2004)
18. R. Bijker, F. Iachello, Phys. Rev. **C69**, 068201 (2004), [nucl-th/0405028](#)
19. P. Mergell, U.G. Meissner, D. Drechsel, Nucl. Phys. **A596**, 367 (1996), [hep-ph/9506375](#)
20. H.W. Hammer, U.G. Meissner, D. Drechsel, Phys. Lett. **B385**, 343 (1996), [hep-ph/9604294](#)
21. H.W. Hammer, U.G. Meissner, Eur. Phys. J. **A20**, 469 (2004), [hep-ph/0312081](#)
22. E. Clementel, C. Villi, Nuovo Cim. **4**, 1207 (1956)
23. S. Bergia et al., Phys. Rev. Lett. **6**, 367 (1961)
24. L.C. Maximon, J.A. Tjon, Phys. Rev. **C62**, 054320 (2000), [nucl-th/0002058](#)
25. P.G. Blunden, W. Melnitchouk, J.A. Tjon, Phys. Rev. Lett. **91**, 142304 (2003), [nucl-th/0306076](#)
26. P.G. Blunden, W. Melnitchouk, J.A. Tjon, Phys. Rev. **C72**, 034612 (2005), [nucl-th/0506039](#)
27. J. Arrington, Phys. Rev. **C71**, 015202 (2005), [hep-ph/0408261](#)
28. Y.M. Bystritskiy, E.A. Kuraev, E. Tomasi-Gustafsson, Phys. Rev. **C75**, 015207 (2007)
29. V. Tvaskis et al., Phys. Rev. **C73**, 025206 (2006), [nucl-ex/0511021](#)
30. R.J. Gould, Astrophys. J. **230**, 967 (1979)
31. V.A. Matveev, R.M. Muradian, A.N. Tavkhelidze, Nuovo Cim. Lett. **7**, 719 (1973)
32. C. Adamuscin, A.Z. Dubnickova, S. Dubnicka, R. Pekarik, P. Weisenpacher, Eur. Phys. J. **C28**, 115 (2003), [hep-ph/0203175](#)
33. H.W. Hammer, D. Drechsel, U.G. Meissner, Phys. Lett. **B586**, 291 (2004), [hep-ph/0310240](#)
34. M.A. Belushkin, H.W. Hammer, U.G. Meissner, Phys. Lett. **B633**, 507 (2006), [hep-ph/0510382](#)
35. M.A. Belushkin, H.W. Hammer, U.G. Meissner, U.G. Meissner (2006), [hep-ph/0608337](#)
36. S.D. Bass, Rev. Mod. Phys. **77**, 1257 (2005), [hep-ph/0411005](#)
37. S.D. Bass, C.A. Aidala, Int. J. Mod. Phys. **A21**, 4407 (2006), [hep-ph/0606269](#)
38. F. Carvalho, F.S. Navarra, M. Nielsen, Phys. Rev. **C72**, 068202 (2005), [nucl-th/0509042](#)
39. D. von Harrach, Prog. Part. Nucl. Phys. **55**, 308 (2005)
40. A.W. Thomas, R.D. Young, Nucl. Phys. **A782**, 1 (2007)
41. M.P. Rekalo, E. Tomasi-Gustafsson, Eur. Phys. J. **A22**, 331 (2004), [nucl-th/0307066](#)

42. V.b. Berestetsky, E.m. Lifshitz, L.p. Pitaevsky (????), Oxford, Uk: Pergamon (1982) 652 P. (Course Of Theoretical Physics, 4)
43. W.M. Yao et al. (Particle Data Group), J. Phys. **G33**, 1 (2006)
44. G.G. Simon, C. Schmitt, F. Borkowski, V.H. Walther, Nucl. Phys. **A333**, 381 (1980)
45. L.E. Price et al., Phys. Rev. **D4**, 45 (1971)
46. C. Berger, V. Burkert, G. Knop, B. Langenbeck, K. Rith, Phys. Lett. **B35**, 87 (1971)
47. R.C. Walker et al., Phys. Rev. **D49**, 5671 (1994)
48. L. Andivahis et al., Phys. Rev. **D50**, 5491 (1994)
49. I.A. Qattan et al., Phys. Rev. Lett. **94**, 142301 (2005), [nucl-ex/0410010](#)
50. M.E. Christy et al. (E94110), Phys. Rev. **C70**, 015206 (2004), [nucl-ex/0401030](#)
51. K.M. Hanson et al., Phys. Rev. **D8**, 753 (1973)
52. G. Hohler et al., Nucl. Phys. **B114**, 505 (1976)
53. T. Janssens et al., Phys. Rev. **142**, 922 (1966)
54. W. Bartel et al., Nucl. Phys. **B58**, 429 (1973)
55. J. Litt et al., Phys. Lett. **B31**, 40 (1970)
56. A.F. Sill et al., Phys. Rev. **D48**, 29 (1993)
57. T. Pospischil et al. (A1), Eur. Phys. J. **A12**, 125 (2001)
58. B.D. Milbrath et al. (Bates FPP), Phys. Rev. Lett. **80**, 452 (1998), [nucl-ex/9712006](#)
59. S. Dieterich et al., Phys. Lett. **B500**, 47 (2001), [nucl-ex/0011008](#)
60. M.K. Jones et al. (Jefferson Lab Hall A), Phys. Rev. Lett. **84**, 1398 (2000), [nucl-ex/9910005](#)
61. G. MacLachlan et al., Nucl. Phys. **A764**, 261 (2006)
62. O. Gayou et al. (Jefferson Lab Hall A), Phys. Rev. Lett. **88**, 092301 (2002), [nucl-ex/0111010](#)
63. C.B. Crawford et al. (2006), [nucl-ex/0609007](#)
64. M.K. Jones et al. (Jefferson Lab Resonance Spin Structure), Phys. Rev. **C74**, 035201 (2006), [nucl-ex/0606015](#)
65. I. Passchier et al., Phys. Rev. Lett. **82**, 4988 (1999), [nucl-ex/9907012](#)
66. H. Zhu et al. (E93026), Phys. Rev. Lett. **87**, 081801 (2001), [nucl-ex/0105001](#)
67. J. Becker et al., Eur. Phys. J. **A6**, 329 (1999)
68. J. Bermuth (A1), AIP Conf. Proc. **603**, 331 (2001)
69. J. Golak, G. Ziemer, H. Kamada, H. Witala, W. Gloeckle, Phys. Rev. **C63**, 034006 (2001), [nucl-th/0008008](#)
70. G. Warren et al. (Jefferson Lab E93-026), Phys. Rev. Lett. **92**, 042301 (2004), [nucl-ex/0308021](#)
71. N. Savvinov (JLab E93-026), Braz. J. Phys. **34**, 717 (2004)
72. D. Rohe et al., Phys. Rev. Lett. **83**, 4257 (1999)
73. J. Bermuth et al., Phys. Lett. **B564**, 199 (2003), [nucl-ex/0303015](#)
74. R. Schiavilla, I. Sick, Phys. Rev. **C64**, 041002 (2001), [nucl-ex/0107004](#)
75. A. Lung et al., Phys. Rev. Lett. **70**, 718 (1993)
76. G. Kubon et al., Phys. Lett. **B524**, 26 (2002), [nucl-ex/0107016](#)
77. H. Anklin et al., Phys. Lett. **B336**, 313 (1994)
78. P. Markowitz et al., Phys. Rev. **C48**, 5 (1993)
79. E.E.W. Bruins et al., Phys. Rev. Lett. **75**, 21 (1995)
80. H. Anklin et al., Phys. Lett. **B428**, 248 (1998)
81. W. Xu et al., Phys. Rev. Lett. **85**, 2900 (2000), [nucl-ex/0008003](#)
82. H. Gao et al., Phys. Rev. **C50**, 546 (1994)
83. W. Xu et al. (Jefferson Lab E95-001), Phys. Rev. **C67**, 012201 (2003), [nucl-ex/0208007](#)
84. S. Rock et al., Phys. Rev. Lett. **49**, 1139 (1982)
85. D.I. Glazier et al., Eur. Phys. J. **A24**, 101 (2005), [nucl-ex/0410026](#)
86. C. Herberg et al., Eur. Phys. J. **A5**, 131 (1999)
87. T. Eden et al., Phys. Rev. **C50**, 1749 (1994)
88. M. Ostrick et al., Phys. Rev. Lett. **83**, 276 (1999)
89. R. Madey et al. (E93-038), Phys. Rev. Lett. **91**, 122002 (2003), [nucl-ex/0308007](#)
90. T. Reichelt et al. (Jefferson Laboratory E93-038), Eur. Phys. J. **A18**, 181 (2003)
91. B. Plaster et al. (Jefferson Laboratory E93-038), Phys. Rev. Lett. **91**, 122002 (2003), [nucl-ex/0511025](#)